




Review

# Green Carbon Dots: Applications in Development of Electrochemical Sensors, Assessment of Toxicity as Well as Anticancer Properties

Madushmita Hatimuria<sup>1</sup>, Plabana Phukan<sup>1</sup> , Soumabha Bag<sup>1</sup> , Jyotirmoy Ghosh<sup>2</sup>, Krishna Gavvala<sup>3</sup>, Ashok Pabbathi<sup>1,\*</sup>  and Joydeep Das<sup>4,\*</sup>

<sup>1</sup> Department of Industrial Chemistry, School of Physical Sciences, Mizoram University, Aizawl 796004, Mizoram, India

<sup>2</sup> Department of Chemistry, Banwarilal Bhalotia College, Asansol 713303, West Bengal, India

<sup>3</sup> Department of Chemistry, Indian Institute of Technology-Hyderabad, Hyderabad 502285, Telangana, India

<sup>4</sup> Department of Chemistry, School of Physical Sciences, Mizoram University, Aizawl 796004, Mizoram, India

\* Correspondence: pabbathi@mzu.edu.in (A.P.); joydeep@mzu.edu.in (J.D.)

**Abstract:** Carbon dots are one of the most promising nanomaterials which exhibit a wide range of applications in the field of bioimaging, sensing and biomedicine due to their ultra-small size, high photostability, tunable fluorescence, electrical properties, etc. However, green carbon dots synthesized from several natural and renewable sources show some additional advantages, such as favorable biocompatibility, wide sources, low cost of production and ecofriendly nature. In this review, we will provide an update on the latest research of green carbon dots regarding their applications in cancer therapy and in the development of electrochemical sensors. Besides, the toxicity assessment of carbon dots as well as the challenges and future direction of research on their anticancer and sensing applications will be discussed.

**Keywords:** green carbon dots; toxicity; electrochemical sensor; anticancer agent; biomedicine



**Citation:** Hatimuria, M.; Phukan, P.; Bag, S.; Ghosh, J.; Gavvala, K.; Pabbathi, A.; Das, J. Green Carbon Dots: Applications in Development of Electrochemical Sensors, Assessment of Toxicity as Well as Anticancer Properties. *Catalysts* **2023**, *13*, 537. <https://doi.org/10.3390/catal13030537>

Academic Editors: Indra Neel Pulidindi, Archana Deokar and Aharon Gedanken

Received: 29 January 2023

Revised: 22 February 2023

Accepted: 2 March 2023

Published: 7 March 2023



**Copyright:** © 2023 by the authors. Licensee MDPI, Basel, Switzerland. This article is an open access article distributed under the terms and conditions of the Creative Commons Attribution (CC BY) license (<https://creativecommons.org/licenses/by/4.0/>).

## 1. Introduction

Carbon-based fluorescent nanoparticles, or carbon dots (CDs), are classified into three main categories, namely carbon nanodots, carbon quantum dots and graphene quantum dots [1]. These three different materials have several applications in various fields [2–4]. In 2004, while purifying single-walled carbon nanotubes (SWCNTs), Xu and colleagues discovered carbon quantum dots (CQDs). This group of carbon allotropes has a particle size of less than 10 nm [5]. Since its discovery, CQDs have attracted the attention of scientists due to their unique properties, such as favorable biocompatibility, low toxicity, large surface-to-volume ratio, stable photoluminescence and excellent hydrophilicity, along with tunable optical and electrical properties [6,7]. CQDs have been used in a wide range of applications, which includes carbon fixation, gas storage, cell biology, cancer imaging, drug administration, etc. [8]. Since its discovery, many synthetic routes for the preparation of CQDs have been established, including green means. Although the green approach to prepare CQDs is advantageous, the as-prepared CQDs offers limited practical applications due to its low fluorescence intensity and single emission wavelength. These shortcomings of green CQDs have been improved later upon incorporating special strategies that enhance the intensity and multicolor emission of CQDs [9].

Recently, green carbon dots (GCDs) have gained immense attention, owing to the availability of plenty of natural resources, excellent photophysical properties of the as-prepared GQDs and several other advantages over the CQDs (Table 1). The natural precursors for GCDs include several plant parts, fruits, amino acids, etc. [10–12]. GCDs are more biocompatible, which makes them highly suitable for a wide variety of biological

applications, including drug delivery, antibacterial and anticancer agents [13–15]. GCDs possess large surface areas due to their small size, which facilitates their applications in sensor development [15,16]. One of the advantages of GCDs is their tunable luminescence intensity and surface area by size control. In addition, the reaction conditions, precursors and surface modifications can also play crucial roles for tuning the properties of GCDs.

**Table 1.** Advantages of GCDs over CQDs.

Applications and Advantages	Green Carbon Dots (GCDs)	Carbon Quantum Dots (CQDs)
Precursors availability	High	Low
Preparation cost	Low	High
Aqueous solubility	Generally high	Generally low
Biocompatibility/therapeutic applications	High	Low
Requirement of additional surface passivation/Doping	Not/Less required	Highly required
Biodegradability	Generally high	Generally low

GCDs have tremendous potential applications in biomedicine and bioimaging [13]. For advancements in biological applications, it is important to test the biocompatibility of GCDs. Several *in vitro* studies have been carried out to test the cytotoxicity of GCDs and found that GCDs have shown low toxicity on different cell types [17–19]. However, studies related to GCDs toxicity evaluation *in vivo* are limited [20,21]. For example, Atchudan et al. [22] evaluated the toxicity of GCDs on *C. elegans* and found low toxicity. GCDs are also reported to be potential anticancer agents [19,23] and are used for bioimaging [21] applications. Although most of the GCDs are highly biocompatible and exhibit low cytotoxicity toward cancer cells, they can be used as an effective drug delivery carrier for various cancerous cells due to their small size, which enable them to be absorbed by the cancer cells easily. Both hydrophilic and hydrophobic anticancer drugs can be loaded on the GCD surface via electrostatic, covalent, hydrophobic or pi-pi stacking interaction, and the drug-loaded GCDs show sustained release pattern of the drug under mildly acidic conditions [24]. Besides, GCDs can also be used for the delivery of hydrophobic photosensitizer molecules and other near infrared active substances into cancer cells for photothermal or photodynamic therapy [25].

Fluorescent GCDs can be employed in the sensing of metal ions and organic compounds [15]. Very recently, GCDs are emerging as an excellent probe in electrochemical sensing applications due to their excellent electronic properties, excellent conductivity, low cost of production, and facile surface modification [15]. The electrical conductivity and stability of GCDs can be tuned by changing precursors or synthesis conditions to obtain desired GCDs for electrochemical sensing applications. GCDs offer high active areas and many hydrophilic functional groups, which are important for electrochemical sensing [4,16]. Because of these attractive properties, carbon dots are widely used in sensing applications as modifiers for the fabrication of electrode materials which can improve the rate of electron transferring process [26–29].

However, there are not many reviews focusing on the toxicity and electrochemical sensing applications of GCDs. Herein, first, we briefly discussed a few of the recent studies regarding the green synthesis and optical properties of GCDs. Thereafter, we summarized the recent literature related to the toxicity of GCDs, anticancer activity and electrochemical sensing applications. We further pointed out the challenges and opportunities for GCDs in toxicity assessment, anticancer and electrochemical applications.

## 2. Green Synthesis Methods and Optical Properties of GCDs

The green synthetic method of carbon dots, also referred as GCD in this review, is carried out by using renewable precursor and solvents that are nontoxic and environ-

mentally benign [14]. Either top-down or bottom-up approaches are mostly adopted for the synthesis of GCDs; however, each method offers unique advantages and challenges. We have reviewed recent bottom-up synthetic methods, such as, microwave pyrolysis, hydrothermal (solvothermal process) and electrochemical etching techniques here. GCDs synthetic routes follow three common steps: (i) high temperature pyrolysis of the carbon sources, which results in (ii) carbonization and nucleation, followed by (iii) surface passivation using stable surfactants. The microwave pyrolysis method is selected for the rapid carbon dot synthesis. On the other hand, the hydrothermal (or solvothermal) method produces isotropic (typically below 10 nm diameter) carbon dots which also offers strong emission properties with high quantum yield (QY). The electrochemical etching-based method to prepare carbon dots is simple and convenient to operate; therefore, it can easily be carried out in the laboratory condition. By using these methods, the sizes of GCDs and its luminescent (PL) performance are easily tailored [8,16,30–32].

Each of the green precursor needed to meet certain requirements to be used in these techniques for the synthesis of desired carbon dots. For instance, the carbohydrates with C:H:O as 1:2:1 and which are easy to dehydrate were selected as carbon dot precursor for hydrothermal synthesis [31]. Therefore, carbohydrates sourced from leaves, roots or flowers, fruits and seeds from plants or plant biomass, such as bark, shells, kernels, peels, etc., were used as green carbon dot source [14].

Huo et al. reported a hydrothermal method for the preparation of GCDs from grapefruits. They prepared three types of GCDs: undoped green carbon dots (UGCDs), UGCDs-peel and nitrogen-doped green carbon dots (N-GCDs) [9]. The three types of GCDs showed size-dependent absorption and emission properties plausibly due to their difference in surface energy states. As the size increases in the UGCDs-peel, it exhibited a red-shifted PL emission compared to others [9]. Size dependency was also reported by Ahmadian Fard Fini et al. in a separate hydrothermal method [33] as shown in the scanning electron microscopy (SEM) image in Figure 1 [33].

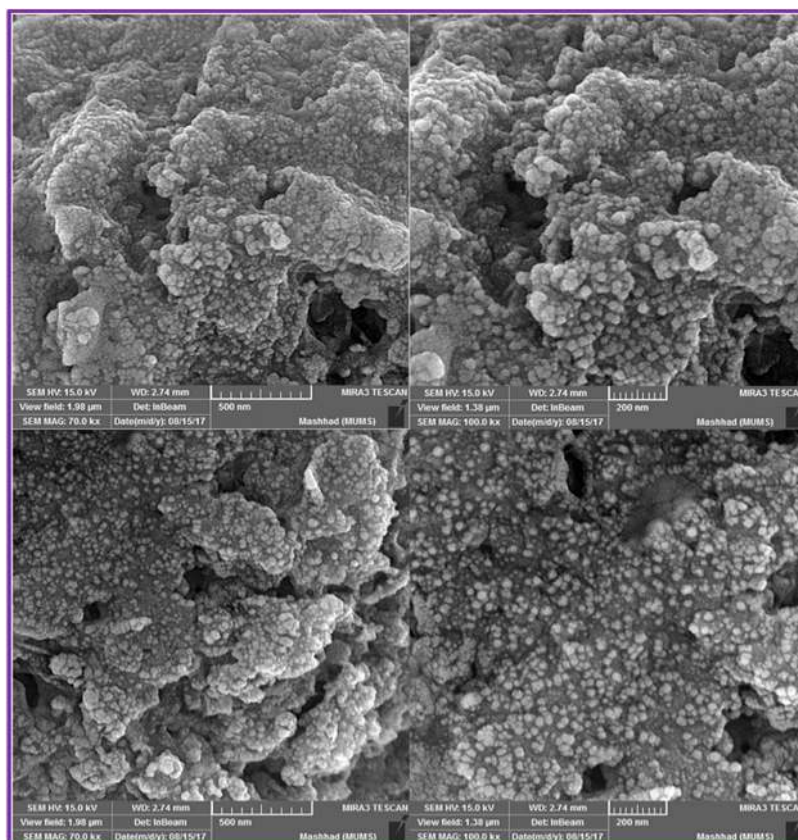


**Figure 1.** SEM images of carbon dots with different sizes. Reproduced with permission from ref. [33].

Zhu et al. decomposed alkali lignin (AL) to GCD through hydrothermal method. As part of the process, the AL were hydrolyzed in presence of mild organic acids (e.g., 4-aminobenzoic acid, benzenesulphonic acid, 4-aminobenzenesulphonic acid, 2,4-diaminobenzenesulphonic acid) before the hydrothermal treatment. These GCDs showed stability in a wide pH range (3–11). They also exhibited yellowish green fluorescence below pH 7 due to the protonation, and green due to deprotonation in basic medium [7]. The emission property also changed with respect to the sizes of the GCDs as shown in Figure 2.

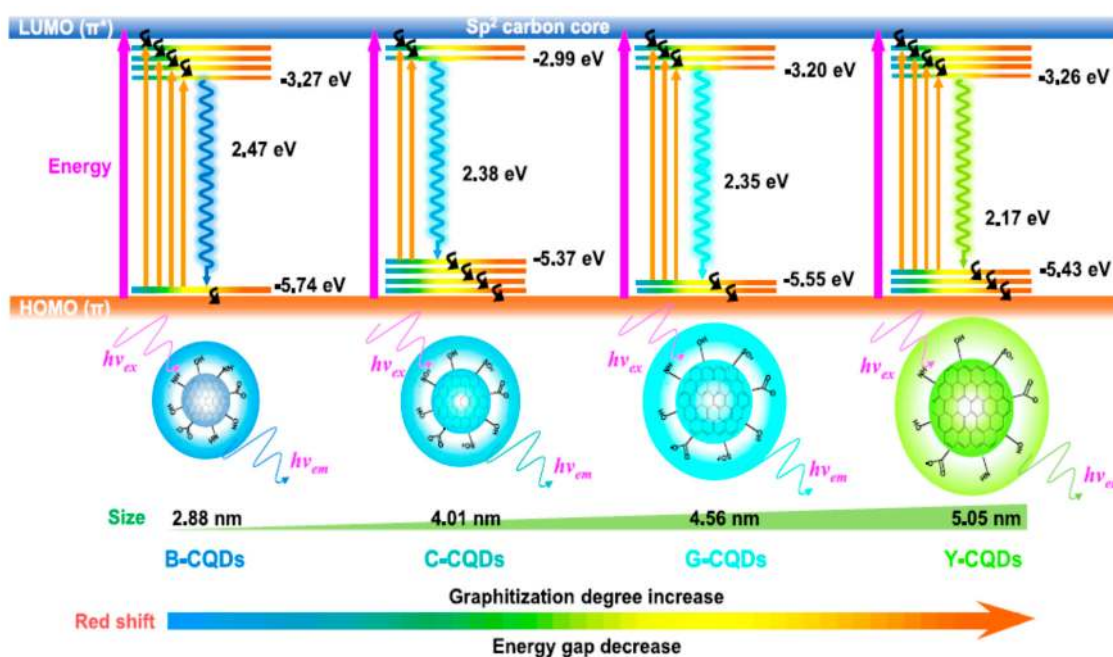


**Figure 2.** Classification of GCD based on their size and emission properties. While smaller GCDs emit blue color, the red shifting of emission occurs as the GCD size increases. Reproduced with permission from Zhu et al. [7].

Zheng et al. used 2,7-dihydroxynaphthalene as the carbon source for the synthesis of GCDs with high product yield through an effective one-step solvothermal method. With a particle size close to 3.31 nm (Table 2), these GCDs offer high quantum yield (QY) [34]. From the results of their study, Zheng et al. found that the red-green-blue (RGB) spectral composition was 93.86% for the GCDs [34].

**Table 2.** GCDs quantum yield (QY) values under different reaction conditions [34].

V(EDA) (mL)	QY%	GCDs Size	Reaction Duration (h)	Reaction Temperature (°C)
0	5.29	3.31 nm	12	180
2	41.07	3.31 nm	12	180
4	62.98	3.31 nm	12	180
8	36.22	3.31 nm	12	180
4	15.07	3.31 nm	12	160
4	62.98	3.31 nm	12	180
4	43.05	3.31 nm	12	200
4	25.42	3.31 nm	10	180
4	62.98	3.31 nm	12	180
4	24.02	3.31 nm	14	180

Hoan et al. reported hydrothermally prepared GCDs from lemon juice (at 120 to 280 °C for 12 h) which were amorphous in nature. Dynamic light scattering measurement confirmed the ~50 nm size of the GCDs. The zeta potential value of the GCDs was ~9.48 mV, confirming that they are relatively stable. Under UV irradiation, the GCD dispersion emits green color. The fluorescence intensity is only influenced by the hydrothermal reaction times (3, 6, 9 and 12 h) as emission increases with the increase in reaction time. Size distribution, band gaps and the excitation-emission wavelength of the as-prepared GCDs are impacted by the reaction temperature as shown in Table 3. Temperature-dependent aggregation and the absence of functional groups contribute toward the properties of the GCDs [31]. Mathew et al. prepared GCDs from *Simarouba glauca* (SG) leaves through hydrothermal method, where the SG leaves are of carbon source. The prepared GCDs showed selective electrochemical sensing properties toward doxycycline [35].

**Table 3.** Quantum yield values of hydrothermally prepared GCDs under different temperature conditions [31].

V <sub>(Lemon Juice)</sub> (mL)	Reaction Temperature (°C)	Reaction Duration (h)	QY%
40	150	12	14.8
40	200	12	16.87
40	240	12	21.37
40	280	12	24.89

In another synthesis of GCDs, Asghar et al. reported the preparation of 2–7 nm GCDs from honey through microwave digestion. As-prepared GCDs showed D (presence of sp<sup>3</sup> defects) and G (in-plane stretching vibration of sp<sup>2</sup> carbon atoms) band in Raman spectrum [36]. Zhao et al. studied blue-emitting GCDs (prepared through hydrothermal method) where they used biomass water hyacinth as a carbon source [37].

Visheratina et al. used *D*- and *L*-cysteine for the preparation of chiral GCDs by hydrothermal carbonization. At the identical hydrothermal condition (150 °C for 4 and 20 h), *L*-GCDs size ranges from 4.4 ± 0.5 to 5.3 ± 0.3 nm, which are all larger in diameter than *D*-GCDs [38].

Yen et al. selected a simple three-electrode (graphite-coated rod, Ag/AgCl reference electrode and platinum (Pt) wire as the counter electrode) electrochemical method to make high-quality GCDs in pure water electrolyte (i.e., in the absence of acids and bases). With the use of this facile electrochemical fabrication, smaller than 5 nm GCD-water suspension could be prepared in a single step, without separate workup, such as filtering, dialysis, centrifugation, column chromatography, or gel-electrophoresis [39]. Summary of the above-mentioned reports are shown in Table 4.

Hydrothermal technique is therefore the most widely used method for the preparation of GCDs because of its easiness, low cost, high scalability and eco-friendly nature. However, in order to bring GCDs into commercial applications, more study should be conducted on the search for high-quality natural precursors for the synthesis of GCDs with improved chemical and photo-stability, which will allow GCDs to become an excellent alternative to existing quantum dots or other dyes for bioimaging applications.

**Table 4.** Size and optical properties of the hydrothermally (solvothermally) prepared GCDs are summarized.

Author	Treatment	GCDs Source	Size (nm)	Excitation Wavelength (nm)	Emission Wavelength (nm)	Ref.
Huo et al.	Hydrothermal	Natural grapefruit	4.74–8.20	320–360	411–420	[9]
Zhu et al.	Hydrolysis followed by hydrothermal	Alkali lignin	2.88–5.05	450	520	[7]
Zheng et al.	Solvothermal	2,7-dihydroxynaphthalene	3.31	460	513	[34]
Hoan et al.	Hydrothermal	Lemon juice	3–5	410–480	500–550	[31]
Mathew et al.	Hydrothermal	Simarouba glauca leaves	2.64	365	445	[35]
Asghar et al.	Microwave	Honey	2–7	-	-	[36]
Visheratina et al.	Hydrothermal	<i>L</i> -cysteine <i>D</i> -cysteine	4.4 and 5.3 4.4 and 5.3	350	~430	[38]
Yen et al.	Electrochemical	Graphite-coated rod	0.5–4	365	500	[39]

### 3. Electrochemical Sensing Ability of GCDs

In the case of GCDs, the smaller the particle size, the more the surface-to-area ration increases, which in turn enhances the contact area in the electrode. This observation makes GCD a good candidate for electrochemical sensing. To study the electrochemical behavior of GCDs, Borna et al. modified the glassy carbon electrode (GCE) with CQDs and used cyclic voltammetry (CV) as well as linear sweep voltammetry (LSV) to detect the anticancer drug, letrozole. In CV, the GCE modified with GCDs exhibit the highest intensity of the anodic and cathodic peak current, plausibly due to the small size of GCDs. The enhanced surface area increased the contact area of the modified electrode with the analyte, and boosted the current intensity. These findings also demonstrate the function of GCDs as an electrocatalyst. In the presence of letrozole, a significant current increase was seen in the modified electrode with electrochemically synthesized GCDs at a current intensity of 100 mA. As a result, the GCE modified with GCDs was chosen as the best electrode for use in the construction of sensors and drug analysis (letrozole analysis) as shown in Table 5 [6].

**Table 5.** Detection limit of different sensors [6].

Sensor	Material	Detection Limit (M)	Sensitivity (A/M)	GCDs Synthesized Method	Required Current for GCDs Synthesis	GCDs Size Range
GCE/GCDs	Letrozole	$1.85 \times 10^{-5}$	0.111	Electrochemical	100 mA	1–10 nm
GCE/GCDs	Clomifene	$70 \times 10^{-5}$	0.041	Electrochemical	100 mA	1–10 nm
GCE/GCDs	Letrozole	$4.23 \times 10^{-5}$	0.076	Electrochemical	200 mA	1–10 nm
GCE/GCDs	Clomifene	$85 \times 10^{-5}$	0.033	Electrochemical	200 mA	1–10 nm
GCE/GCDs	Letrozole	$5.15 \times 10^{-5}$	0.067	Electrochemical	300 mA	1–10 nm
GCE/GCDs	Clomifene	$90 \times 10^{-5}$	0.028	Electrochemical	300 mA	1–10 nm
GCE/GCDs	Letrozole	$4.27 \times 10^{-5}$	0.069	Hydrothermal	-	1–10 nm
GCE/GCDs	Clomifene	$87 \times 10^{-5}$	0.031	Hydrothermal	-	1–10 nm

Zhou et al. reported an increase in oxidation efficiency of ascorbic acid (AA) using NH<sub>2</sub>-GCDs-modified GCE. The NH<sub>2</sub>-GCDs could increase the conductivity of the electrode surface, and the positively charged amine groups allow them to interact with the dienol hydroxyl groups in AA through electrostatic contact, thereby detecting AA with a high degree of specificity. They found that, compared to many other previously reported

quantum dot materials, the NH<sub>2</sub>-GCDs had a superior effect on detecting AA in both electrochemistry and fluorescence approaches. It is due to this reason that the NH<sub>2</sub>-GCDs is able to boost the rate of electron transfer via direct connection with diene hydroxyl groups in AA. Additionally, NH<sub>2</sub>-GCDs can also be joined to AA by hydrogen bonds [40].

Ran et al. used WP6-N-GCD (water soluble pillar [6] arenes nitrogen-doped green carbon dot) nanocomposite as an electrode material to build a sensitive electrochemical sensing platform for trinitrotoluene (TNT) detection. The electrochemical analysis demonstrated that WP6-N-GCDs outperformed the  $\beta$ -CD-N-GCDs in terms of supramolecular recognition and enrichment capabilities, and displayed a higher peak current toward TNT. The WP6-N-GCD-modified electrode showed a linear response ranging from 0.001  $\mu$ M to 1  $\mu$ M and from 1  $\mu$ M to 20  $\mu$ M with a LOD of 0.95 nM due to the synergistic effects of WP6 and N-GCDs. These results indicate that WP-N-GCD composites are ideal materials for electrochemical sensing platforms as shown in Table 6 [41].

**Table 6.** Comparison of some electrode materials for electrochemical sensing of TNT [41].

Materials	Linear Range ( $\mu$ M)	LOD (nM)
Ionic liquid-graphene	0.13–6.6	17.6
Boron-doped diamond	0.088–1.76	44
Ordered mesoporous carbon	-	0.88
Nitrogen-doped graphene	0.53–8.8	129.9
Deposited graphene	0.0044–0.88	0.88
N-rich carbon nanodots	5–30	1
PtPd-rGONRs	0.044–13.2	3.5
Vanadium dioxide	0.44–4.4	4.4
N-doped graphene nanodots	0.0044–1.76	0.88
WP6-N-GCDs	0.001–1; 1–20	0.95

GCDs have also been used to determine hydrogen peroxide (H<sub>2</sub>O<sub>2</sub>), a common industrial oxidant electrochemically. Hassanvand et al. [16] demonstrated the use of GCE modified with GCDs as an amperometric H<sub>2</sub>O<sub>2</sub> sensor. When compared to octahedral Cu<sub>2</sub>O, GCDs/octahedral Cu<sub>2</sub>O exhibited more favorable electrocatalysis behavior for the glucose oxidation and H<sub>2</sub>O<sub>2</sub> reduction reactions, as shown in Table 7 [16].

**Table 7.** H<sub>2</sub>O<sub>2</sub> and glucose detection by GCDs-based electrochemical sensors [16].

Modified Electrode	Target Compounds	Detection Limit	GCD Size	Electrochemical Method
GCDs/GCE	H <sub>2</sub> O <sub>2</sub>	$3 \times 10^{-9}$ M	-	Amperometry
GCDs/Cu <sub>2</sub> O/NF/GCE	H <sub>2</sub> O <sub>2</sub>	$2.8 \times 10^{-6}$ M	10 nm	Amperometry
CuO/GCDs/CHNS/GCE	H <sub>2</sub> O <sub>2</sub>	$2.4 \times 10^{-9}$ M	~4–6 nm	Amperometry
GCDs/Cu <sub>2</sub> O/GCE	Glucose	$6 \times 10^{-6}$ M	-	Amperometry
GCDs/AuNPs-GOx/Au	Glucose	$17 \times 10^{-6}$ M	-	Amperometry
GCDs/Au-NPs-Gox/GDAE	Glucose	$13.6 \times 10^{-6}$ M	-	Amperometry

Accurate clinical dopamine (DA) diagnosis can help to address several neurological disorders. Modifying GCE with N-doped green carbon dots (NGCDs) can be used for DA detection with a wide linear range and a low detection limit, as shown in Table 8 [16].

**Table 8.** DA detection using different GCDs-based sensors [16].

Modified Electrode	Method	Target Compound	GCDs Average Size	Detection Limit
GCDs/MoS <sub>2</sub> /Mo foil	CV	DA	-	0.0090 μM
NF/NGCDs/GCE	DPV	DA	7.4 nm	1.0 nM
GCDs/GCE	LSV	DA	3.3 nm	2.7 μM
β-CD/GCDs/GCE	DPV	DA	7.6 nm	0.14 μM

Wang et al. have shown that when GCDs are mixed separately with layered-double-hydroxides (LDHs), metal sulfides, and metal phosphides, etc., they can be used as electrocatalysts for oxygen reduction reaction (ORR), oxygen evolution reaction (OER), hydrogen evolution reaction (HER), CO<sub>2</sub> reduction reaction (CO<sub>2</sub>RR), etc. OER activity of CoP/GCDs composite is better with 400 mV overpotential in alkaline electrolytes than pure CoP. The CoP/GCDs composite's electrical catalytic performance is increased due to the presence of functional groups, its small size, good conductivity, and fast electron transfer of GCDs. If specific surface area is high, the presence of electrochemical active sites will be high, and contact area with the electrolyte will be large, which results in increasing HER performance [30].

Lin et al. [15] described the potential use of GCDs as electrochemical sensors as it can be synthesized through different methods, have rich functional groups, and can make composites with other materials easily. When GCE was modified with GCDs, it showed an increase in response current and potential compared to bare GCE. It also showed a greater electrochemical reaction due to the presence of many functional groups in GCDs/GCE [15]. When Mathew et al. compared the bare GCE and the developed ternary sensor, they found that the anodic peak current becomes threefold in the case of the developed ternary sensor. This shows that the developed ternary sensor was able to detect small levels of doxycycline accurately. They conducted the electrochemical sensing in phosphate buffer solution, where the potential range was 0 to 1 V for cyclic voltametric measurement, with a scan rate of 50 mV/s. The modified GCE was remarkably stable and had great repeatability and reusability [35].

From the above discussion, it is clear that GCDs are widely used for the sensitive and selective detection of a large number of biomolecules, such as ascorbic acids, hydrogen peroxide, drug molecules, as well as explosives (trinitrotoluene). However, only limited studies are reported till date. Therefore, more research should be conducted to explore the potential applications of GCDs.

#### 4. Toxicity Assessment and Anticancer Properties of Green Carbon Dots (GCDs)

GCDs synthesized from various green sources have many potential biological applications. Here, we will discuss about the biocompatibility of these synthesized GCDs studied by several researchers with normal and cancerous cells.

Ensafi et al. prepared fluorescent carbon dots from a naturally sourced saffron. Cytotoxicity of saffron carbon dots was tested on olfactory mucosa cells and bone marrow cells after incubating for 24 h, and low toxicity for all the different concentrations (Table 9) of carbon dots was observed [42]. Zhang et al. prepared green carbon dots using schizonepetae herba carbonisata (SHC). Cytotoxicity of the prepared carbon dots was evaluated in RAW 264.7 cells in various concentrations (Table 9). Cell viability was negligible, but with increasing concentration from 840–10,000 μg/mL, cell viability started to decrease [10].



**Table 9.** Toxicity of GCDs for normal cells.

Sl No.	Material	Source of Green Carbon Dot Synthesis	Average Size (nm)	Toxicity Assay in Cell Line	Concentration	Remark	Reference
1	Fluorescent carbon dots	Saffron	6.0	Olfactory mucosa cells and bone marrow cells	0.005–1.5 mg/mL	Low toxicity (more than 70% cell viability remains)	[42]
2	Carbon dots	Schizonepetae herba carbonisata (SHC)	0.8–4.0	RAW 264.7 cells	39.06–10,000 µg/mL	Negligible cytotoxicity up to 840 µg/mL concentration	[10]
3	Carbon dots	Phellodendri cortex (PC)	1.2–4.8	RAW 264.7 cells	0.01–10,000 µg/mL	Negligible cytotoxicity up to 1000 µg/mL concentration	[17]
4	Enantiomeric carbon dots	L-lysine D-lysine	4.0	SH-SY5Y cells	0.2 and 0.4 mg/mL	L-lysine carbon dots showed negligible cytotoxicity	[12]
5	Carbon dots	Gum tragacanth (GT) Gum tragacanth (GT) and chitosan	70–90	Human umbilical vein endothelial cells (HUVEC cell line)	0–50 µg/mL	Low cytotoxicity (more than 80% cell viability remains)	[18]
6	Re-based carbon dots	Ginsenoside Re, citric acid and EDA	4.6	Human renal epithelial cells 293T, HL-7702 (L-02), MCF-10A and NSFbs	0–1.0 mg/mL	Low toxicity (after 24 h of incubation, cell viability was more than 90%)	[23]
7	Fluorescent carbon dots	Cinnamon	3.4	Human kidney cells (HK-2)	0.1–2.0 mg/mL	Low toxicity (more than 80% cell viability remains)	[19]
		Red chili	3.1		0.1–2.0 mg/mL		
		Turmeric	4.3		0.1–2.0 mg/mL		
		Black pepper	3.5		0.1–4.0 mg/mL		
8	Carbon dots	Kiwi	4.4	Epithelial human kidney cells (HK-2)	0.25–5.0 mg/mL	Low toxicity (up to 1 mg/mL concentration cell viability more than 60%)	[11]
		Avocado	4.4				
		Pear	4.1				
9	Fluorescent NP-carbon dots	Wet algal biomass	4.7	HEK-293 (normal human embryonic kidney cell line)	5–75 µg/mL	Negligible cytotoxicity	[43]
10	Fluorescent carbon dots	Cyanobacteria powder	2.5	PC12 cells	0–1000 µg/mL	Low cytotoxicity	[44]
11	Carbon dots	Banana peel waste	5	Nematode	0–200 µg/mL	Negligible cytotoxicity	[45]
12	Carbon dots	<i>Fusobacterium nucleatum</i> cells	4.1	BEAS-2B (Lung normal epithelial cells)	12.5–200 µg/mL	Low cytotoxicity (more than 80% cell viability remains)	[46]
13	Fluorescent carbon dots	Fresh mint leaves	6.5	Primary H8 cells	0–200 µg/mL	Negligible cytotoxicity	[47]
14	Carbon dots (CDs)	E-CD Citric acid and EDA	10	EA. hy926 cells	0.1–3.2 mg/mL	Low cytotoxicity	[48]
		U-CD Urea and citric acid	5				

From the natural source of Phellodendri cortex (PC), Liu and his coworkers prepared green carbon dots. Cytotoxicity of these green carbon dots was evaluated in RAW 264.7 cells with eight different concentrations (Table 9). After 24 h of incubation, cell viability was negligible by up to 1000 µg/mL of concentration. However, when the concentration increased to more than that amount, cytotoxicity also started to increase [17]. Malishev et al. prepared two types of green carbon dots using amino acids (Table 9) as a natural source. Cytotoxicity of these amino acid-based carbon dots was evaluated in SH-SY5Y cells. For the cytotoxicity assay, Aβ42 was induced in both types of the carbon dots. Cytotoxicity was measured for Aβ42 alone and Aβ42-induced carbon dots. Without carbon dots, in the presence of Aβ42, cell viability decreased to 25%. In the case of pre-incubated Aβ42 with D-lysine carbon dots at the above concentrations (Table 9), the results did not show much difference with Aβ42 alone. However, in the case of pre-incubated Aβ42 with L-lysine carbon dots at both the concentrations (Table 9), the results have shown significantly low cytotoxicity [12].

Two types of green carbon dots (GT carbon dots and GT/Chitosan carbon dots) were prepared by Moradi and his coworkers using natural and ecofriendly sources, gum

tragacanth and chitosan. Cytotoxicity of these prepared carbon dots was tested in human umbilical vein endothelial cells (HUVEC cell line) at different concentrations (Table 9) after 24 h of incubation, and low cytotoxicity and high biocompatibility were observed [18].

Carbon dots prepared from natural sources (Table 9) were used by Yao and his coworkers to evaluate the cytotoxicity assay in human renal epithelial cells 293T, HL-7702(L-02), MCF-10A and NSFbs. After 24 h of incubation of the cell lines with various concentrations (Table 9) of prepared carbon dots, they observed low cytotoxicity for all the concentrations [23].

Vasimalai et al. prepared four different types of carbon dots from four different spices, i.e., cinnamon, red chili, turmeric and black pepper. Cytotoxicity of these prepared carbon dots were evaluated in different concentrations (Table 9) on human kidney cells (HK-2) after 24 h of incubation. For all the carbon dots, cell viability remained at more than 80% at 0–2.0 mg/mL concentration, but in the case of black pepper carbon dots at higher concentrations (3.0 and 4.0 mg/mL), results showed high toxicity for the cell line [19]. Cytotoxicity of these four carbon dots in different concentrations on HK-2 and LN229 cells is shown in the Figure 3.

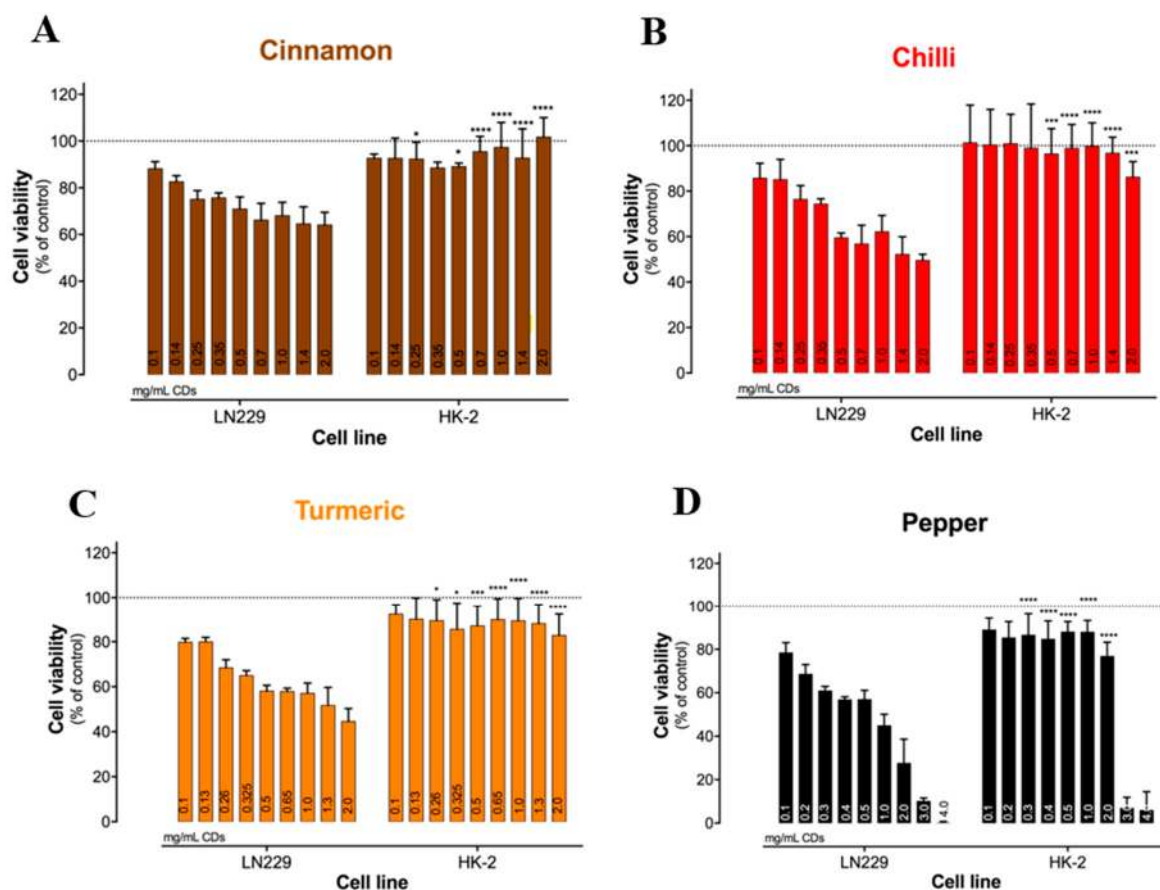


**Figure 3.** Cell viability evaluation in two different types of cells (cancerous LN229 cells and normal HK-2 cells) after a 24 h incubation with increasing concentrations of: (A) cinnamon, (B) red chili, (C) turmeric and (D) black pepper carbon dots. Represented results are mean  $\pm$  SD of at least three independent experiments. \*  $p < 0.05$ , \*\*\*  $p < 0.001$  and \*\*\*\*  $p < 0.0001$  are for statistical significance of differences between the effect of the same concentration of spice-based carbon dots in other cell line (LN229). Adapted from ref. [19].

Fruit-based carbon dots were prepared by Dias and his team from kiwi, avocado and pear. For the cytotoxicity evaluation at different concentrations (Table 9) of the prepared carbon dots, epithelial human kidney cell (HK-2) line was used. Cells were incubated for two different time periods (48 and 72 h) with different concentrations of carbon dots. After

72 h of incubation, cell viability was more than that measured at 48 h. When concentration is more than 1 mg/mL, cell viability started to decrease. Overall, pear-based carbon dots showed more cell viability and kiwi-based carbon dots showed less cell viability [11]. Wet algal biomass source was used by Singh and his coworker to prepare green carbon dots. HEK-293 (normal human embryonic kidney) cell line was used for the cytotoxicity evaluation of these carbon dots. After 24 h of incubation in different concentrations of carbon dots (Table 9), more than 80% of cell viability was observed, even in the highest concentration (Table 9) [43]. Wang et al. evaluated the cytotoxicity of cyanobacteria-based carbon dots in PC12 cells in different concentrations (Table 9), and 94.4% of cell viability was observed, up to 100 µg/mL concentration. Even at a high concentration (500 µg/mL), cell viability was observed to be more than 80%, which concludes low cytotoxicity and biocompatibility [44].

From the banana peel waste, Atchudan and his team prepared green carbon dots, and for the cytotoxicity evaluation in different concentrations (Table 9), live-cell line (nematode) was used. From their observations, overall, only 5% cell viability was decreased even at the highest concentration, thereby indicating negligible cytotoxicity with excellent biocompatibility [45]. Liu et al. prepared carbon dots from *Fusobacterium nucleatum* cells, and a cytotoxicity test was evaluated in BEAS-2B (lung normal epithelial cells) cell line. After incubation for 48 h at different carbon dots concentrations (Table 9), low cytotoxicity was observed for all concentrations [46]. From fresh mint leaves, Raveendran and Kizhakayil prepared green carbon dots and performed a cytotoxicity assay with different concentrations (Table 9) in primary H8 cells. For all the concentrations, no significant change was observed in cell viability [47].

Cytotoxicity of curcumin-loaded green carbon dots (Curc-GCDs) and prepared GCDs were studied in different concentrations (Table 9) by Arvapalli et al. [48] in EA. hy926 cells. They prepared two different types of carbon dots (Table 9) and then loaded the carbon dots with curcumin. Their observations showed very low cytotoxicity for both Curc-GCDs and GCDs at EA. hy926 cells, even at the highest concentration (Table 9) after 24 h of incubation [48].

Most of the GCDs mentioned in the list had shown excellent biocompatibility in the normal cells. Therefore, all the green sources used in Table 9 has great potential toward GCDs preparation. However, most of the studies used low concentrations for the cytotoxicity evaluation. Thus, future studies should focus on toxicity evaluation using a wide range of concentrations.

Most of the prepared GCDs mentioned in Table 10 showed low toxicity and excellent biocompatibility in all the cancerous cells. Chatzimitakos et al. [49] prepared GCDs from two different green sources (Table 10) and studied the cytotoxicity of prepared GCDs in various cancerous cells (Table 10). Results showed that after 48 h of incubation, cell viability for citrus sinensis CD and citrus limon CD is more than 90% and 95%, respectively [49]. GCDs prepared from green sources (water chestnut and onion) were used by Hu and his team to evaluate the cytotoxicity in the cancerous cell (Table 10) and observed low cytotoxicity in all the concentrations (Table 10) [50].

Among all the discussed literature in Table 10, only limited GCDs showed cytotoxicity toward some selected cancer cells and are therefore useful for cancer therapy. Yao et al. prepared carbon dots from natural sources (Ginsenoside Re, citric acid and EDA) to evaluate their toxicity in cancer cell lines, i.e., HepG2, MCF-7 and A375 cells and normal cells (Table 9). After 24 h of incubation with various concentrations (Table 10) of prepared carbon dots, they observed that with increasing concentrations, cell viability decreased to 50%, 40% and 30% for HepG2, MCF-7 and A375 cells, respectively. A375 cells showed the highest inhibition than other cells. Further LDH-release assay and ROS generation was checked in A375 cells. From the LDH-release assay, they observed a concentration-dependent LDH release in the medium. When compared to the normal cell, ROS generation was comparatively high in cancer cells, thereby causing oxidative damage and apoptosis in the cancer cells. Therefore, these carbon dots can be considered as potential anticancer agents [23].

**Table 10.** Toxicity assay of GCDs for cancerous cells.

Sl No.	Material	Source of Green Carbon Dot Synthesis	Average Size (nm)	Toxicity Assay in Cell Line	Concentration	Remark	Reference
1	Luminescent carbon dots	Citrus sinensis	6.5	HeLa, A549, MDA-MB-231 and HEK-293 cells	400 µg/mL	Extremely low cytotoxicity	[49]
		Citrus limon peels	4.5				
2	S and N co-doped carbon dots	Water chestnut and onion	3.5	Human bladder cancer T24 cells	0–300 µg/mL	Low cytotoxicity (after 24 h of incubation, cell viability remained at more than 80% for all the concentrations)	[50]
3	Nitrogen- and sulfur-co-doped carbon dots	Ginkgo leaves juice	2.2	HeLa cells	N/A	Low cytotoxicity	[51]
4	NIR-light emission carbon dots	Fresh spinach	3–11	A549 cells	0–200 µg/mL	Negligible toxicity (after 24 h of co-incubation, cell viability showed above 94.2% at all the concentrations)	[52]
5	Multicolor luminescent carbon dots	ATP	3.8	HeLa cells	0–500 µg/mL	Negligible toxicity (very less change was observed between 24 h and 48 h incubation)	[53]
6	N-doped carbon dots	Sucrose and urea	1.6	HeLa cells	0–1.0 mg/mL	Negligible cytotoxicity (cell viability was more than 98.5% after 24 h of incubation, even at a high concentration, i.e., 1.0 mg/mL)	[54]
7	Hydrophilic carbon dots	Glucose powder	2.6	HeLa cells	0–1.0 mg/mL	Negligible cytotoxicity (cell viability was more than 98% after 24 h of incubation, even at a high concentration, i.e., 1.0 mg/mL)	[55]
8	Carbon dots	Date kernels	2.5	Human MG-63 cells	200.0 µg/mL	Low cytotoxicity (after 48 h of incubation, cell viability remains more than 85%)	[56]
9	Carbon dots	Quince fruit ( <i>Cydonia oblonga</i> ) powder	4.9	HT-29 cells	5–1000 µg/mL	Low toxicity	[57]
10	Re-based carbon dots	Ginsenoside Re, citric acid and EDA	4.6	MCF-7, A375 HepG2 cells	0–1.0 mg/mL	High cytotoxicity * While carbon dots were prepared separately from Ginsenoside; citric acid and EDA, cytotoxicity was relatively low.	[23]
11	Fluorescent carbon dots	Cinnamon	3.4	Human glioblastoma cells (LN-229 cancer cell line)	0.1–2.0 mg/mL	High toxicity	[19]
		Red chili	3.1		0.1–2.0 mg/mL		
		Turmeric	4.3		0.1–2.0 mg/mL		
		Black pepper	3.5		0.1–4.0 mg/mL		
12	Carbon dots	Kiwi	4.4	Epithelial human colorectal adenocarcinoma cells (Caco-2)	0.25–5.0 mg/mL	Low toxicity (below 1.5 mg/mL concentration, cell viability was more than 80%, but cell death can induce in higher concentrations)	[11]
		Avocado	4.4				
		Pear	4.1				
13	Fluorescent carbon dots	<i>Prunus cerasifera</i> fruits juice	3–5	HepG2 cells	0–500 µg/mL	Low toxicity (after 24 h of incubation below 500 µg/mL concentration, cell viability was more than 90%)	[58]
14	Carbon dots	Celery leaves	2.1	HepG2 cells	0.01–0.022 g/mL	Low toxicity (cell viability was more than 85% for all the concentration after 24 h of incubation)	[59]
15	Carbon dots	Lychee waste	3.1	A375 (Skin melanoma) cells	0.0–1.2 mg/mL	Low cytotoxicity (after 48 h of incubation, cell viability was more than 89% for the highest concentration, i.e., 1.2 mg/mL)	[60]

Table 10. Cont.

Sl No.	Material	Source of Green Carbon Dot Synthesis	Average Size (nm)	Toxicity Assay in Cell Line	Concentration	Remark	Reference
16	Fluorescent-N-doped carbon dots	Lemon juice and ethylenediamine	3.0	Human breast adenocarcinoma (MCF7) cells	0.312–2.0 mg/mL	Low cytotoxicity (after 24 h of incubation cell viability for 2.0 mg/mL, the highest concentration was more than 88%)	[61]
17	Fluorescent carbon dots	Fresh lamb	At 200 °C = 2.8 At 300 °C = 1.9 At 350 °C = 1.7	HepG2 cells	2.0 mg/mL	Low cytotoxicity (after 4 h of incubation cell viability was more than 90% at this particular concentration)	[62]
18	Carbon dots	<i>Osmanthus fragrans</i> flowers	2.2	A549 cells	25–1000 µg/mL	Negligible toxicity (after 24 h of incubation, cell viability showed above 90% at all concentrations)	[63]
19	Carbon dots	Dried wheat straw	2.1	HeLa cells	0–0.8 mg/mL	Negligible cytotoxicity (cell viability remains more than 90% at all concentrations)	[64]
20	Carbon dots	Gelatin and papain	3.8	A549 cells	0–300 µg/mL	Negligible cytotoxicity (very less difference between 12 h and 24 h incubation for all concentrations, after 24 h incubation, cell viability remained above 91%)	[65]
21	Carbon dots	Glucose	3.0	HeLa, HepG2 and HEK-293 cells	0–300 mg/L	Negligible cytotoxicity (no change in cell viability for HeLa and HepG2 cells, but in the case of HEK-293 cell with increasing concentration, cell viability also increases)	[66]
22	N, B co-doped bright fluorescent carbon dots	<i>Solanum betaceum</i> ( <i>S. betaceum</i> ) fruit extract	5.0	HeLa cells	10–50 µg/mL	Low cytotoxicity (at minimum and maximum concentration, i.e., 10 µg/mL and 50 µg/mL, cell viability were 100% and 70%, respectively)	[67]
23	Carbon dots	Gelatin	5.0	MCF-7 cell line	20–120 µg/mL	Low cytotoxicity (cell viability was more than 80% even for the highest concentration after 24 h of incubation)	[68]
24	Zwitterionic carbon dots	Citric acid and L-histidine	8.5	A549 cells	0.01–1.5 mg/mL	Low cytotoxicity (after 24 h of incubation, cell viability was more than 90% even at a high concentration)	[69]
25	Carbon dots	Corn stalk shell	1.2–3.2	A549 cells	0–100 mg/L	Low cytotoxicity (after incubation for 24 h, cell viability remained more than 90% for all concentrations. Again, after 48 h of incubation, cell viability remained more than 75% for 100 mg/L concentration)	[70]
26	Carbon dots	<i>Fusobacterium nucleatum</i> cells	4.1	HeLa cells	12.5–200 µg/mL	Low cytotoxicity (more than 80% cell viability remains)	[46]
27	Nitrogen-doped carbon dots	Jackfruit peel (JFP) Tamarind peel (TP)	6.4 5.3	Dalton's lymphoma ascites cells (DLA)	50–200 µg/mL	Low cytotoxicity only in low concentrations, i.e., below 50 µg/mL (at 200 µg/mL concentration for JFP-carbon dots 100%, cell death was observed, but in the case of TP-carbon dots, only 60% cell death happened)	[71]
28	Carbon dots	Arginine, chitosan, citric acid	6–11	AGS cells	30:1–70:1 (carrier/DNA)	Negligible toxicity (at highest weight, cell viability decreased to 90%)	[72]
29	Folic acid-functionalized carbon dots	Red Korean ginseng	70	MCF-7 cells	10–50 µg/mL	High toxicity after 48 h of incubation	[73]

Table 10. Cont.

Sl No.	Material	Source of Green Carbon Dot Synthesis	Average Size (nm)	Toxicity Assay in Cell Line	Concentration	Remark	Reference
30	Carbon dots	Tea leaves	200	HepG2 cells	0–160 µg/mL	Low cytotoxicity (more 90% cell viability after 24 h of incubation at all concentrations)	[74]
31	Carbon dots	<i>Simarouba glauca</i> leaf	2.6	Human breast cancer cell line (MCF-7)	0–100 µg/mL	High toxicity with increasing concentration	[35]
32	Carbon dots	Walnut oil	12.3	PC3, MCF-7, and HT-29 cells	0–10 µg/mL	High cytotoxicity after 24 h of incubation	[75]
33	Carbon dots (CDs)	E-CDs Citric acid and EDA	10.0	HepG2 and A549 cells	0.1–3.2 mg/mL	High cellular toxicity with increasing concentration	[48]
		U-CDs Urea and citric acid	5.0				

Four types of natural carbon dots were prepared by Vasimalai and his team using four different spices (Table 10). Toxicity assay was performed after 24 h of incubation in human glioblastoma cells (LN-229 cancer cell line) with various concentrations (Table 10). A significant decrease was observed in cell viability for all the concentrations of carbon dots (Figure 3). At 2.0 mg/mL concentration, 35%, 50% and 75% reduction in cell viability was observed for cinnamon, red chili and turmeric, and black pepper-derived carbon dots, respectively. In the case of black pepper-derived carbon dots, cell viability reduced to 100% at the highest concentration (Table 10) [19]. Tejwan et al. studied the anticancer property of rutin drug loaded with folic acid-functionalized carbon dots (FA-CDs-RUT) extracted from ginseng root in MCF-7 cells. After 48 h of incubation in different concentrations (Table 10) of FA-CDs-RUT, CDs and RUT were compared with each other for anticancer property. Moreover, results showed that in the presence of rutin drug in the carbon dots (FA-CDs-RUT), anticancer property was found to be more in MCF-7 cells than in CDs and RUT drug alone. Furthermore, they observed that intracellular ROS generation was increased with subsequent cellular apoptosis when the cells were treated with FA-CDs-RUT nanohybrid [73].

Mathew et al. [35] studied the anticancer activity of carbon dots prepared from naturally occurring *Simarouba glauca* (*S. glauca*) leaf. Cell viability of prepared GCDs was tested with different concentrations (Table 10), and cellular morphologies were also checked in human breast cancer cell line (MCF-7). They observed that cell viability decreased with an increasing concentration of the GCDs. After 24 h of incubation at the highest concentration (Table 10), complete cell death was observed. Arkan et al. [75] studied the anticancer property of prepared GCDs (Table 10) in three different cancerous cells (PC3, MCF-7 and HT-29). After 24 h of incubation in various concentrations (Table 6), 50% of cell death was observed for PC3 and MCF-7 at 1.25 µg/mL and 5 µg/mL concentration, respectively, indicating that walnut oil-based carbon dots have anticancer property. However, there was no cell death observed in the case of HT-29 cell lines. At the highest concentration, cell viability was also observed to be more than 70% for HT-29 cell lines.

Arvapalli et al. [48] prepared two different types of GCDs (E-CDs and U-CDs) loaded with curcumin and then compared the GCDs with curcumin-loaded carbon dots (Curc-GCDs) to test the cell viability in HepG2 and A549 cells. Incubation was performed for 24 h in different concentrations (Table 10) of GCDs and Curc-GCDs. They found that, compared to synthesized GCDs, Curc-GCDs showed more toxicity to the cells. In HepG2 cells, cell viability was decreased to 40% and 30% at the highest concentration (Table 10) when the cells were treated with Curc-E-GCDs and Curc-U-GCDs, respectively. In A549 cell, cell viability was decreased even more than HepG2 at the same concentration to 38% and 18% when treated with Curc-E-GCDs and Curc-U-GCDs, respectively. In both cases,

Curc-U-GCDs showed higher toxicity to the cells. Furthermore, when the cell viability test was extended up to 48 h and 72 h for A549 cells at the same concentration, they observed that, in the presence of Curc-E-GCDs, cell viability decreased to 30% and 25%, and in the presence of Curc-U-GCDs, cell viability decreased to 5% and 2%, respectively [48].

From the above discussion, we can propose that GCDs are mostly biocompatible toward most of the cancer cell lines and display only negligible cytotoxicity. Besides, the size-dependent toxicity measurement was also not reported so far for both cancerous and non-cancerous cells. However, when the GCDs are conjugated with several anticancer drug molecules, they could increase the drug stability in biological media and its concentration in the target organ, thereby increasing the pharmacological action of the drug. Therefore, more research should be conducted to establish GCDs as an efficient drug delivery vehicle.

## 5. Conclusions

Carbon dots are one of the fascinating nanomaterials with a broad range of applications. Taking environmental importance into account, GCDs are considered as promising nanomaterials since the past decade and are very crucial for a sustainable future. As we discussed in this review, due to their unique biological and physico-chemical properties, carbon dots can be used in several applications, including electro-chemical sensors, bioimaging, nanomedicine, in drug delivery and in cancer therapy. In this review, we specifically focused on GCDs and their applications. Although several reports on GCDs are already documented, the research with GQDs is still in the initial phase. However, the following points need to be addressed to further explore the sensing and anticancer applications of GCDs:

1. In order to bring GCDs into commercial applications, more study should be conducted on the search for high-quality natural precursors for their synthesis.
2. In vivo toxicity studies are limited, hence, more in vivo studies involving GCDs should be considered for the implementation of GCDs in biological/clinical applications.
3. In addition, toxicity of GCDs prepared from different natural sources under different synthesis conditions should be investigated to obtain comprehensive details on GCDs toxicity.
4. Future studies should focus on evaluating the anticancer activity of GCDs using in vivo models.
5. More research should be conducted to explore the possibility of using GCDs in photodynamic and photothermal therapy.
6. GCDs-based sensors should also be used for the sensitive and selective detection of cancer biomarkers, such as miRNA and antigens, to explore the application of GCDs in clinical cancer diagnosis.
7. It is also important to check the effect of GCDs' size and surface modifications on anticancer as well as electrochemical sensing abilities.

**Author Contributions:** Conceptualization, A.P., J.D. and S.B.; writing—original draft preparation, M.H. and P.P.; writing—review and editing, M.H., J.G., S.B. and K.G.; supervision, A.P., S.B. and J.D. All authors have read and agreed to the published version of the manuscript.

**Funding:** This research received no external funding.

**Data Availability Statement:** Not applicable.

**Acknowledgments:** M.H. would like to thank DST, INDIA for DST-INSPIRE fellowship (Award number: IF210147). A.P. would like to thank DST, INDIA for the research grant in DST-INSPIRE Faculty Scheme (Award number: IFA20-CH-333). S.B. would like to acknowledge SERB, DST, Govt. of India for Start-up Research Grant (Grant number: SRG/2022/002245). P.P. thanks SERB, DST, Govt. of India for her research fellowship.

**Conflicts of Interest:** The authors declare no conflict of interest.

## References

1. Nazri, N.A.A.; Azeman, N.H.; Luo, Y.; Bakar, A.A.A. Carbon quantum dots for optical sensor applications: A review. *Opt. Laser Technol.* **2021**, *139*, 106928. [[CrossRef](#)]
2. Wang, B.; Wang, M.; Liu, F.; Zhang, Q.; Yao, S.; Liu, X.; Huang, F. Ti<sub>3</sub>C<sub>2</sub>: An Ideal Co-catalyst? *Angew. Chem. Int. Ed.* **2020**, *59*, 1914–1918. [[CrossRef](#)] [[PubMed](#)]
3. Chen, Z.-L.; Wang, D.; Wang, X.-Y.; Yang, J.-H. Enhanced formaldehyde sensitivity of two-dimensional mesoporous SnO<sub>2</sub> by nitrogen-doped graphene quantum dots. *Rare Met.* **2021**, *40*, 1561–1570. [[CrossRef](#)]
4. Yan, J.; Ye, F.; Dai, Q.; Ma, X.; Fang, Z.; Dai, L.; Hu, C. Recent progress in carbon-based electrochemical catalysts: From structure design to potential applications. *Nano Res. Energy* **2023**, *2*, e9120047. [[CrossRef](#)]
5. De Oliveira, B.P.; Da Silva Abreu, F.O.M. Carbon quantum dots synthesis from waste and by-products: Perspectives and challenges. *Mater. Lett.* **2021**, *282*, 128764. [[CrossRef](#)]
6. Borna, S.; Sabzi, R.E.; Pirsá, S. Synthesis of carbon quantum dots from apple juice and graphite: Investigation of fluorescence and structural properties and use as an electrochemical sensor for measuring letrozole. *J. Mater. Sci. Mater. Electron.* **2021**, *32*, 10866–10879. [[CrossRef](#)]
7. Zhu, L.; Shen, D.; Wang, Q.; Luo, K.H. Green synthesis of tunable fluorescent carbon quantum dots from lignin and their application in anti-counterfeit printing. *ACS Appl. Mater. Interfaces* **2021**, *13*, 56465–56475. [[CrossRef](#)] [[PubMed](#)]
8. Desmond, L.J.; Phan, A.N.; Gentile, P. Critical overview on the green synthesis of carbon quantum dots and their application for cancer therapy. *Environ. Sci. Nano.* **2021**, *8*, 848. [[CrossRef](#)]
9. Huo, X.; He, Y.; Ma, S.; Jia, Y.; Yu, J.; Li, Y.; Cheng, Q. Green synthesis of carbon dots from grapefruit and its fluorescence enhancement. *J. Nanomater.* **2020**, *2020*, 8601307. [[CrossRef](#)]
10. Zhang, M.; Zhao, Y.; Cheng, J.; Liu, X.; Wang, Y.; Yan, X.; Zhang, Y.; Lu, F.; Wang, Q.; Qu, H.; et al. Novel carbon dots derived from schizonepetae herba carbonisata and investigation of their haemostatic efficacy. *Artif. Cells Nanomed. Biotechnol.* **2017**, *46*, 1562–1571. [[CrossRef](#)]
11. Dias, C.; Vasimalai, N.; Sarria, M.P.; Pinheiro, I.; Vilas-Boas, V.; Peixoto, J.; Espina, B. Biocompatibility and bioimaging potential of fruit-based carbon dots. *Nanomaterials* **2019**, *9*, 199. [[CrossRef](#)] [[PubMed](#)]
12. Malishev, R.; Arad, E.; Bhunia, S.K.; Shaham-Niv, S.; Kolusheva, S.; Gazit, E.; Jelinek, R. Chiral modulation of amyloid beta fibrillation and cytotoxicity by enantiomeric carbon dots. *Chem. Commun.* **2018**, *54*, 7762–7765. [[CrossRef](#)] [[PubMed](#)]
13. Su, W.; Wu, H.; Xu, H.; Zhang, Y.; Li, Y.; Li, X.; Fan, L. Carbon dots: A booming material for biomedical applications. *Mater. Chem. Front.* **2020**, *4*, 821–836. [[CrossRef](#)]
14. Chahal, S.; Macairan, J.-R.; Yousefi, N.; Tufenkji, N.; Naccache, R. Green synthesis of carbon dots and their applications. *RSC Adv.* **2021**, *11*, 25354–25363. [[CrossRef](#)]
15. Lin, X.; Xiong, M.; Zhang, J.; He, C.; Ma, X.; Zhang, H.; Kuang, Y.; Yang, M.; Huang, Q. Carbon dots based on natural resources: Synthesis and applications in sensors. *Microchem. J.* **2021**, *160*, 105604. [[CrossRef](#)]
16. Hassanvand, Z.; Jalali, F.; Nazari, M.; Parnianchi, F.; Santoro, C. Carbon nanodots in electrochemical sensors and biosensors: A review. *ChemElectroChem* **2021**, *8*, 15–35. [[CrossRef](#)]
17. Liu, X.; Wang, Y.; Yan, X.; Zhang, M.; Zhang, Y.; Cheng, J.; Lu, F.; Qu, H.; Wang, Q.; Zhao, Y.; et al. Novel phellodendri cortex (Huang Bo)-derived carbon dots and their hemostatic effect. *Nanomedicine* **2018**, *13*, 391–405. [[CrossRef](#)]
18. Moradi, S.; Sadrjavadi, K.; Farhadian, N.; Hosseinzadeh, L.; Shahlaei, M. Easy synthesis, characterization and cell cytotoxicity of green nano carbon dots using hydrothermal carbonization of gum tragacanth and chitosan bio-polymers for bioimaging. *J. Mol. Liq.* **2018**, *259*, 284–290. [[CrossRef](#)]
19. Vasimalai, N.; Vilas-Boas, V.; Gallo, J.; de Fátima Cerqueira, M.; Menendez-Miranda, M.; Costa-Fernandez, J.M.; Dieguez, L.; Espina, B.; Fernandez-Arguelles, M.T. Green synthesis of fluorescent carbon dots from spices for in vitro imaging and tumour cell growth inhibition. *Beilstein J. Nanotechnol.* **2018**, *9*, 530–544. [[CrossRef](#)]
20. Chan, M.-H.; Chen, B.-G.; Ngo, L.T.; Huang, W.-T.; Li, C.-H.; Liu, R.-S.; Hsiao, M. Natural carbon nanodots: Toxicity assessment and theranostic biological application. *Pharmaceutics* **2021**, *13*, 1874. [[CrossRef](#)]
21. Wang, B.; Cai, H.; Waterhouse, G.I.N.; Qu, X.; Yang, B.; Lu, S. Carbon dots in bioimaging, biosensing and therapeutics: A comprehensive review. *Small Sci.* **2022**, *2*, 2200012. [[CrossRef](#)]
22. Atchudan, R.; Edison, T.N.J.I.; Perumal, S.; Vinodh, R.; Lee, Y.R. Multicolor-emitting carbon dots from malus floribunda and their interaction with caenorhabditis elegans. *Mater. Lett.* **2020**, *261*, 127153. [[CrossRef](#)]
23. Yao, H.; Li, J.; Song, Y.; Zhao, H.; Wei, Z.; Li, X.; Jin, Y.; Yang, B.; Jiang, J. Synthesis of ginsenoside Re-based carbon dots applied for bioimaging and effective inhibition of cancer cells. *Int. J. Nanomed.* **2018**, *13*, 6249–6264. [[CrossRef](#)]
24. Tejwan, N.; Saha, S.K.; Das, J. Multifaceted applications of green carbon dots synthesized from renewable sources. *Adv. Colloid Interface Sci.* **2020**, *275*, 102046. [[CrossRef](#)] [[PubMed](#)]
25. Tejwan, N.; Saini, A.K.; Sharma, A.; Singh, T.A.; Kumar, N.; Das, J. Metal-doped and hybrid carbon dots: A comprehensive review on their synthesis and biomedical applications. *J. Control. Release* **2021**, *330*, 132–150. [[CrossRef](#)]



26. Karimian, N.; Fakhri, H.; Amidi, S.; Hajian, A.; Arduini, F.; Bagheri, H. A novel sensing layer based on metal–organic framework UiO-66 modified with TiO<sub>2</sub>-graphene oxide: Application to rapid, sensitive and simultaneous determination of paraoxon and chlorpyrifos. *New J. Chem.* **2019**, *43*, 2600–2609. [[CrossRef](#)]
27. Hashemi, P.; Karimian, N.; Khoshshafar, H.; Arduini, F.; Mesri, M.; Afkhami, A.; Bagheri, H. Reduced graphene oxide decorated on Cu/CuO-Ag nanocomposite as a high-performance material for the construction of a non-enzymatic sensor: Application to the determination of carbaryl and fenamiphos pesticides. *Mat. Sci. Eng. C* **2019**, *102*, 764–772. [[CrossRef](#)] [[PubMed](#)]
28. Wang, Q.; Pang, H.; Dong, Y.; Chi, Y.; Fu, F. Colorimetric determination of glutathione by using a nanohybrid composed of manganese dioxide and carbon dots. *Microchim. Acta* **2018**, *185*, 291. [[CrossRef](#)] [[PubMed](#)]
29. Hashemi, P.; Bagheri, H.; Afkhami, A.; Amidi, S.; Madrakian, T. Graphene nanoribbon/FePt bimetallic nanoparticles/uric acid as a novel magnetic sensing layer of screen printed electrode for sensitive determination of ampyra. *Talanta* **2018**, *176*, 350–359. [[CrossRef](#)]
30. Wang, X.; Feng, Y.; Dong, P.; Huang, J. A mini review on carbon quantum dots: Preparation, properties, and electrocatalytic application. *Front. Chem.* **2019**, *7*, 671. [[CrossRef](#)]
31. Hoan, B.T.; Tam, P.D.; Pham, V.-H. Green synthesis of highly luminescent carbon quantum dots from lemon Juice. *J. Nanotechnol.* **2019**, *2019*, 2852816. [[CrossRef](#)]
32. Anwar, S.; Ding, H.; Xu, M.; Hu, X.; Li, Z.; Wang, J.; Liu, L.; Jiang, L.; Wang, D.; Dong, C.; et al. Recent advances in synthesis, optical properties, and biomedical applications of carbon dots. *ACS Appl. Bio. Mater.* **2019**, *2*, 2317–2338. [[CrossRef](#)]
33. Ahmadian-Fard-Fini, S.; Salavati-Niasari, M.; Ghanbari, D. Hydrothermal green synthesis of magnetic Fe<sub>3</sub>O<sub>4</sub>-carbon dots by lemon and grape fruit extracts and as a photoluminescence sensor for detecting of *E. coli* bacteria. *Spectrochim. Acta-A Mol. Biomol. Spectrosc.* **2018**, *203*, 481–493. [[CrossRef](#)] [[PubMed](#)]
34. Zheng, J.; Xie, Y.; Wei, Y.; Yang, Y.; Liu, X.; Chen, Y.; Xu, B. An efficient synthesis and photoelectric properties of green carbon quantum dots with high fluorescent quantum yield. *Nanomaterials* **2020**, *10*, 82. [[CrossRef](#)] [[PubMed](#)]
35. Mathew, S.; Thara, C.R.; John, N.; Mathew, B. Carbon dots from green sources as efficient sensor and as anticancer agent. *J. Photochem. Photobiol. A Chem.* **2023**, *434*, 114237. [[CrossRef](#)]
36. Asghar, K.; Qasim, M.; Das, D. One-pot green synthesis of carbon quantum dot for biological application. In *AIP Conference Proceedings*; AIP Publishing LLC: Melville, NY, USA, 2017; Volume 1832, p. 050117.
37. Zhao, P.; Zhang, Q.; Cao, J.; Qian, C.; Ye, J.; Xu, S.; Zhang, Y.; Li, Y. Facile and green synthesis of highly fluorescent carbon quantum dots from water hyacinth for the detection of ferric iron and cellular imaging. *Nanomaterials* **2022**, *12*, 1528. [[CrossRef](#)] [[PubMed](#)]
38. Visheratina, A.; Hesami, L.; Wilson, A.K.; Baalbaki, N.; Noginova, N.; Noginov, M.A.; Kotov, N.A. Hydrothermal synthesis of chiral carbon dots. *Chirality* **2022**, *34*, 1503–1514. [[CrossRef](#)]
39. Yen, Y.-C.; Lin, C.-C.; Chen, P.-Y.; Ko, W.-Y.; Tien, T.-R.; Lin, K.-J. Green synthesis of carbon quantum dots embedded onto titanium dioxide nanowires for enhancing photocurrent. *R. Soc. Open Sci.* **2017**, *4*, 161051. [[CrossRef](#)] [[PubMed](#)]
40. Zhou, X.; Qu, Q.; Wang, L.; Li, L.; Li, S.; Xia, K. Nitrogen doped carbon quantum dots as one dual function sensing platform for electrochemical and fluorescent detecting ascorbic acid. *J. Nanopart. Res.* **2020**, *22*, 20. [[CrossRef](#)]
41. Ran, X.; Qu, Q.; Qian, X.; Xie, W.; Li, S.; Li, L.; Yang, L. Water-soluble pillar [6]arene functionalized nitrogen-doped carbon quantum dots with excellent supramolecular recognition capability and superior electrochemical sensing performance towards TNT. *Sens. Actuators B Chem.* **2018**, *257*, 362–371. [[CrossRef](#)]
42. Ensafi, A.A.; Sefat, S.H.; Kazemifard, N.; Rezaei, B.; Moradi, F. A novel one-step and green synthesis of highly fluorescent carbon dots from saffron for cell imaging and sensing of prilocaine. *Sens. Actuators B Chem.* **2017**, *253*, 451–460. [[CrossRef](#)]
43. Singh, A.K.; Singh, V.K.; Singh, M.; Singh, P.; Khadim, S.R.; Singh, U.; Koch, B.; Hasan, S.H.; Asthana, R.K. One pot hydrothermal synthesis of fluorescent NP-carbon dots derived from dunaliella salina biomass and its application in on-off sensing of Hg (II), Cr (VI) and live cell imaging. *J. Photochem. Photobiol. A Chem.* **2019**, *376*, 63–72. [[CrossRef](#)]
44. Wang, X.; Yang, P.; Feng, Q.; Meng, T.; Wei, J.; Xu, C.; Han, J. Green preparation of fluorescent carbon quantum dots from cyanobacteria for biological imaging. *Polymers* **2019**, *11*, 616. [[CrossRef](#)] [[PubMed](#)]
45. Atchudan, R.; Edison, T.N.J.I.; Shanmugam, M.; Perumal, S.; Somanathan, T.; Lee, Y.R. Sustainable synthesis of carbon quantum dots from banana peel waste using hydrothermal process for in vivo bioimaging. *Phys. E Low-Dimens. Syst. Nanostruct.* **2020**, *126*, 114417. [[CrossRef](#)]
46. Liu, L.; Zhang, S.; Zheng, X.; Li, H.; Chen, Q.; Qin, K.; Ding, Y.; Wei, Y. Carbon dots derived from *fusobacterium nucleatum* for intracellular determination of Fe<sup>3+</sup> and bioimaging both in vitro and in vivo. *Anal. Methods* **2021**, *13*, 1121–1131. [[CrossRef](#)] [[PubMed](#)]
47. Raveendran, V.; Kizhakayil, R.N. Fluorescent carbon dots as biosensor, green reductant, and biomarker. *ACS Omega* **2021**, *6*, 23475–23484. [[CrossRef](#)] [[PubMed](#)]
48. Arvapalli, D.M.; Sheardy, A.T.; Allado, K.; Chevva, H.; Yin, Z.; Wei, J. Design of curcumin loaded carbon nanodots delivery system: Enhanced bioavailability, release kinetics, and anticancer activity. *ACS Appl. Bio Mater.* **2020**, *3*, 8776–8785. [[CrossRef](#)] [[PubMed](#)]

49. Chatzimitakos, T.; Kasouni, A.; Sygellou, L.; Avgeropoulos, A.; Troganis, A.; Stalikas, C. Two of a kind but different: Luminescent carbon quantum dots from citrus peels for iron and tartrazine sensing and cell imaging. *Talanta* **2017**, *175*, 305–312. [[CrossRef](#)]
50. Hu, Y.; Zhang, L.; Li, X.; Liu, R.; Lin, L.; Zhao, S. Green preparation of S and N co-doped carbon dots from water chestnut and onion as well as their use as an off-on fluorescent probe for the quantification and imaging of coenzyme A. *ACS Sustain. Chem. Eng.* **2017**, *5*, 4992–5000. [[CrossRef](#)]
51. Li, L.; Wang, X.; Fu, Z.; Cui, F. One-step hydrothermal synthesis of nitrogen- and sulfur-co-doped carbon dots from ginkgo leaves and application in biology. *Mater. Lett.* **2017**, *196*, 300–303. [[CrossRef](#)]
52. Li, L.; Zhang, R.; Lu, C.; Sun, J.; Wang, L.; Qu, B.; Li, T.; Liu, Y.; Li, S. In situ synthesis of NIR-light emitting carbon dots derived from spinach for bio-imaging applications. *J. Mater. Chem. B* **2017**, *5*, 7328–7334. [[CrossRef](#)] [[PubMed](#)]
53. Zhang, M.; Chi, C.; Yuan, P.; Su, Y.; Shao, M.; Zhou, N. A hydrothermal route to multicolor luminescent carbon dots from adenosine disodium triphosphate for bioimaging. *Mater. Sci. Eng. C* **2017**, *76*, 1146–1153. [[CrossRef](#)] [[PubMed](#)]
54. Liu, X.; Liu, J.; Zheng, B.; Yan, L.; Dai, J.; Zhuang, Z.; Du, J.; Guo, Y.; Xiao, D. N-doped carbon dots: Green and efficient synthesis on a large-scale and their application in fluorescent pH sensing. *New J. Chem.* **2017**, *41*, 10607–10612. [[CrossRef](#)]
55. Liu, X.; Yang, C.; Zheng, B.; Dai, J.; Yan, L.; Zhuang, Z.; Du, J.; Guo, Y.; Xiao, D. Green anhydrous synthesis of hydrophilic carbon dots on large-scale and their application for broad fluorescent pH sensing. *Sens. Actuators B Chem.* **2017**, *255*, 572–579. [[CrossRef](#)]
56. Amin, N.; Afkhami, A.; Hosseinzadeh, L.; Madrakian, T. Green and cost-effective synthesis of carbon dots from date kernel and their application as a novel switchable fluorescence probe for sensitive assay of zoledronic acid drug in human serum and cellular imaging. *Anal. Chim. Acta* **2018**, *1030*, 183–193. [[CrossRef](#)] [[PubMed](#)]
57. Ramezani, Z.; Qorbanpour, M.; Rabhar, N. Green synthesis of carbon quantum dots using quince fruit (*Cydonia oblonga*) powder as carbon precursor: Application in cell imaging and As<sup>3+</sup> determination. *Colloids Surf. A Physicochem. Eng. Asp.* **2018**, *549*, 58–66. [[CrossRef](#)]
58. Ma, H.; Sun, C.; Xue, G.; Wu, G.; Zhang, X.; Han, X.; Qi, X.; Lv, X.; Sun, H.; Zhang, J.; et al. Facile synthesis of fluorescent carbon dots from *prunus cerasifera* fruits for fluorescent ink, Fe<sup>3+</sup> ion detection and cell imaging. *Spectrochim. Acta-A Mol. Biomol. Spectrosc.* **2019**, *213*, 281–287. [[CrossRef](#)]
59. Qu, Y.; Yu, L.; Zhu, B.; Chai, F.; Su, Z. Green synthesis of carbon dots by celery leaves for use as fluorescent paper sensors for the detection of nitrophenols. *New J. Chem.* **2019**, *44*, 1500–1507. [[CrossRef](#)]
60. Sahoo, N.K.; Jana, G.C.; Aktara, M.N.; Das, S.; Nayim, S.; Patra, A.; Bhattacharjee, P.; Bhadra, K.; Hossain, M. Carbon dots derived from lychee waste: Application for Fe<sup>3+</sup> ions sensing in real water and multicolor cell imaging of skin melanoma cells. *Mater. Sci. Eng. C* **2019**, *108*, 110429. [[CrossRef](#)]
61. Tadesse, A.; Hagos, M.; RamaDevi, D.; Basavaiah, K.; Belachew, N. Fluorescent-nitrogen-doped carbon quantum dots derived from citrus lemon juice: Green synthesis, mercury(II) ion sensing, and live cell imaging. *ACS Omega* **2020**, *5*, 3889–3898. [[CrossRef](#)]
62. Wang, H.; Xie, Y.; Na, X.; Bi, J.; Liu, S.; Zhang, L.; Tan, M. Fluorescent carbon dots in baked lamb: Formation, cytotoxicity and scavenging capability to free radicals. *Food Chem.* **2019**, *286*, 405–412. [[CrossRef](#)]
63. Wang, M.; Wan, Y.; Zhang, K.; Fu, Q.; Wang, L.; Zeng, J.; Xia, Z.; Gao, D. Green synthesis of carbon dots using the flowers of *osmanthus fragrans* (Thunb.) Lour. as precursors: Application in Fe<sup>3+</sup> and ascorbic acid determination and cell imaging. *Anal. Bioanal. Chem.* **2019**, *411*, 2715–2727. [[CrossRef](#)]
64. Liu, S.; Liu, Z.; Li, Q.; Xia, H.; Yang, W.; Wang, R.; Li, Y.; Zhao, H.; Tian, B. Facile synthesis of carbon dots from wheat straw for colorimetric and fluorescent detection of fluoride and cellular imaging. *Spectrochim. Acta-A Mol. Biomol. Spectrosc.* **2020**, *246*, 118964. [[CrossRef](#)] [[PubMed](#)]
65. Li, C.; Sun, X.; Li, Y.; Liu, H.; Long, B.; Xie, D.; Chen, J.; Wang, K. Rapid and green fabrication of carbon dots for cellular imaging and anti-counterfeiting applications. *ACS Omega* **2021**, *6*, 3232–3237. [[CrossRef](#)] [[PubMed](#)]
66. Liu, Y.-Y.; Yu, N.-Y.; Fang, W.-D.; Tan, Q.-G.; Ji, R.; Yang, L.-Y.; Wei, S.; Zhang, X.-W.; Miao, A.-J. Photodegradation of carbon dots cause cytotoxicity. *Nat. Commun.* **2021**, *12*, 812. [[CrossRef](#)]
67. Arul, V.; Chandrasekaran, P.; Sivaraman, G.; Sethuraman, M.G. Efficient green synthesis of N,B co-doped bright fluorescent carbon nanodots and their electrocatalytic and bio-imaging applications. *Diam. Relat. Mater.* **2021**, *116*, 108437. [[CrossRef](#)]
68. Choppadandi, M.; Guduru, A.T.; Gondaliya, P.; Arya, N.; Kalia, K.; Kumar, H.; Kapusetti, G. Structural features regulated photoluminescence intensity and cell internalization of carbon and graphene quantum dots for bioimaging. *Mater. Sci. Eng. C* **2021**, *129*, 112366. [[CrossRef](#)]
69. Emami, E.; Mousazadeh, M.H. pH-responsive zwitterionic carbon dots for detection of rituximab antibody. *Luminescence* **2021**, *36*, 1198–1208. [[CrossRef](#)]
70. Li, Z.; Wang, Q.; Zhou, Z.; Zhao, S.; Zhong, S.; Xu, L.; Gao, Y.; Cui, X. Green synthesis of carbon quantum dots from corn stalk shell by hydrothermal approach in near-critical water and applications in detecting and bioimaging. *Microchem. J.* **2021**, *166*, 106250. [[CrossRef](#)]
71. Paul, A.; Kurian, M. Facile synthesis of nitrogen doped carbon dots from waste biomass: Potential optical and biomedical applications. *Clean. Eng. Technol.* **2021**, *3*, 100103. [[CrossRef](#)]
72. Rezaei, A.; Hashemi, E. A pseudohomogeneous nanocarrier based on carbon quantum dots decorated with arginine as an efficient gene delivery vehicle. *Sci. Rep.* **2021**, *11*, 13790. [[CrossRef](#)] [[PubMed](#)]

73. Tejwan, N.; Sadhukhan, P.; Sharma, A.; Singh, T.A.; Hatimutia, M.; Pabbathi, A.; Das, J.; Sil, P.C. pH-responsive and targeted delivery of rutin for breast cancer therapy via folic acid-functionalized carbon dots. *Diam. Relat. Mater.* **2022**, *129*, 109346. [[CrossRef](#)]
74. He, Z.; Cheng, J.; Yan, W.; Long, W.; Ouyang, H.; Hu, X.; Liu, M.; Zhou, N.; Zhang, X.; Wei, Y.; et al. One-step preparation of green tea ash derived and polymer functionalized carbon quantum dots via the thiol-ene click chemistry. *Inorg. Chem. Commun.* **2021**, *130*, 108743. [[CrossRef](#)]
75. Arkan, E.; Barati, A.; Rahmanpanah, M.; Hosseinzadeh, L.; Moradi, S.; Hajialyani, M. Green synthesis of carbon dots derived from walnut oil and an investigation of their cytotoxic and apoptogenic activities toward cancer cell. *Adv. Pharm. Bull.* **2018**, *8*, 149–155. [[CrossRef](#)] [[PubMed](#)]

**Disclaimer/Publisher's Note:** The statements, opinions and data contained in all publications are solely those of the individual author(s) and contributor(s) and not of MDPI and/or the editor(s). MDPI and/or the editor(s) disclaim responsibility for any injury to people or property resulting from any ideas, methods, instructions or products referred to in the content.